ISSN 1392–1320 MATERIALS SCIENCE (MEDŽIAGOTYRA). Vol. 23, No. 4. 2017

Ti and Nb Addition to Ni_3Al: Site Preferences and Alloying Efficiency from First Principles Calculations

Haiguang RUAN [1], **Fuxiang HUANG** [1] *, **Zhaochao ZHANG** [1], **Zhiqian CHEN** [2]

[1] *College of Materials Science and Engineering, Chongqing University of Technology, Chongqing, 400054, China*
[2] *Faculty of Materials and Energy, Southwest University, Chongqing, 400715, China*

http://dx.doi.org/10.5755/j01.ms.23.4.17051

Received 29 November 2016; accepted 17 April 2017

The first principles calculations were performed to investigate site preferences of the alloying elements M (Ti, Nb) doping in Ni_3Al, elastic properties and the electronic structure of Ni_3Al and Ni_3Al-M with the Cambridge sequential total energy package (CASTEP). It was found that M were preferred to replace the Al sites. As the M doping. The bulk, shear and Young's modulus increased and the bulk/shear modulus ratios (B/G) decreased in Ni_3Al polycrystalline alloy. While B/G of all alloys were larger than 1.75, signifying that Ni_3Al, $Ni_{24}Al_7Nb$ and $Ni_{24}Al_7Ti$ polycrystalline alloys possessed ductility. Analyzing the electronic structure of Ni_3Al and Ni_3Al-M, the results showed that the main interaction between the Ni atoms and the Al atoms was covalence in the Ni_3Al, after doping elements M (Ti, Nb) in Ni_3Al, there was strong orbital hybridization between the Al-3p orbital, Ni-3d orbital and M-d (Ti-3d, Nb-4d) orbital, the covalent bonds between alloying atoms M (Ti, Nb) and their neighbor atoms Ni were stronger than that between Al atom and Ni atom.

Keywords: first principles calculations, site preferences, elastic properties, electronic structure.

1. INTRODUCTION

As one of Ni-based superalloys, Ni_3Al-based alloys are very important for their application in turbine engines, the transportation, etc., and have the following character-istics: good high-temperature oxidation resistance, high temperature creep resistance, high work hardening rate at room temperature, thus they are hopeful to become good high temperature structural materials [1 – 4]. The good properties of Ni_3Al-based alloys are mainly owned to Ni_3Al (γ' phase). As an ordered phase, the yield strength of which increases with increases of temperature below 880°C. Recently, the researches about Ni_3Al-based alloys were focused on the experiments and the theoretical calculation for the γ′-Ni_3Al.

In the experiments, alloying elements in Ni_3Al alloy tend to form complex compounds and improve the mechanical properties. For example, Aoki et al. [5] reported that B on the Ni-rich site improved the ductility of binary Ni_3Al alloy or ternary Ni_3Al alloyed with each element (Zr, Hf, V, Nb, MO, W, Co, Pd, Cu, Cr, Mn and Fe). Soga [6], Tomihisa K [7] reported that the elements (Nb, Ti, Zr, V, Hf and Cr) increased high temperature strength of Ni_3Al alloys. In theoretical calculation, First-principles theory has been widely applied in alloying efficiency on doped Ni_3Al. Q.Wu et al. [8 – 11] reported that the effects of alloying elements (Mo, Re, Ta, W, Ti, Co, Nb, Ru, Cr, Y) on the elastic properties of Ni_3Al, and the synergistic effect of Mo-Ta, Mo-Re and Mo-Cr co-alloying elements on site preferences and elastic properties of Ni_3Al have been further computed [12].

M (Ti, Nb) are transition metals, and the radius and electronegativity of which are similar to the Al. When added into the Ni_3Al alloy, they replace the Al sites [13], and forming the Ni_3Ti and Ni_3Nb, which are high strength phases at high temperature. Thus the effects of M (Ti, Nb) added into the Ni_3Al have been studied in the experiments and the theoretical calculations as above. Unfortunately, previous studies had been conducted to research elastic properties of Ni_3Al-M (Ti, Nb) ternary alloys, and few reported electronic structure of M (Ti, Nb) in Ni_3Al alloy, such as Soga [6] and Q. Wu [8]. In this work, the site preferences of the alloying elements X in Ni_3Al and elastic properties of Ni_3Al alloys are predicted with the first-principles theory. Moreover, the density of states, electron density difference and Mulliken population of Ni_3Al and Ni_3Al-M are analyzed, and which also can be used to explain elastic properties change of Ni_3Al with M (Ti, Nb) doping.

2. CALCULATION MODEL AND METHODS

Ni_3Al cell has the variant structure of FCC and belongs to an ordered $L1_2$ structure [14], where the Ni atoms occupy the site of the face center and the Al atoms occupy the site of the cube corner. The arrangement of atoms in space is illustrated in Fig. 1. The lattice parameters are $a = b = c = 3.572$ Å, $\alpha = \beta = \gamma = 90$ for Ni_3Al crystal cell, and the space group of which is PM-3M [15]. As shown in Fig. 2, the supercells with a 2×2×2 arrangement of Ni_3Al crystal cell has 32 atoms, and are used to predict site preferences of alloying elements X (Ni, Ti and Nb) in Ni_3Al, the concentration of X is 3.125 at % in each supercell.

In the present study, all calculations, including the elastic constants, the total energy and the electric structures, are performed with the Cambridge sequential total energy package (CASTEP) based on the density functional theory [16]. The exchange–correlation functional between the electrons is described with Perdew-Burke-Ernzerhof (PBE) of generalized gradient

---

* Corresponding author. Tel.: +86-23-68667787.
E-mail address: *hfuxiang@163.com* (F.X. Huang)

approximation (GGA) [17]. The ultrasoft pseudopotential Plane-Wave with cut off energy of 360 eV are taken into account in the simulation, and a 6×6×6 Monkhorst-Pack k-mesh is used for Sampling of the irreducible wedge of the Brillouin zone in reciprocal space. The spin-polarization are adopted for all calculations. The convergence tolerance of geometry optimization calculations with Broyden-Flecher-Goldfarb-Shanno (BFGS) [18] before all calculations is 5×10^{-7} eV/atom for energy, and the maximum force tolerance is 1.00×10^{-2} eV/Å per atom.

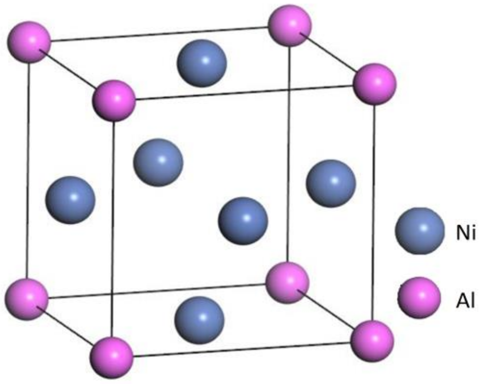

Fig. 1. Original model of Ni_3Al crystal cell, the structure symmetry is a = b = c, α = β = γ = 90

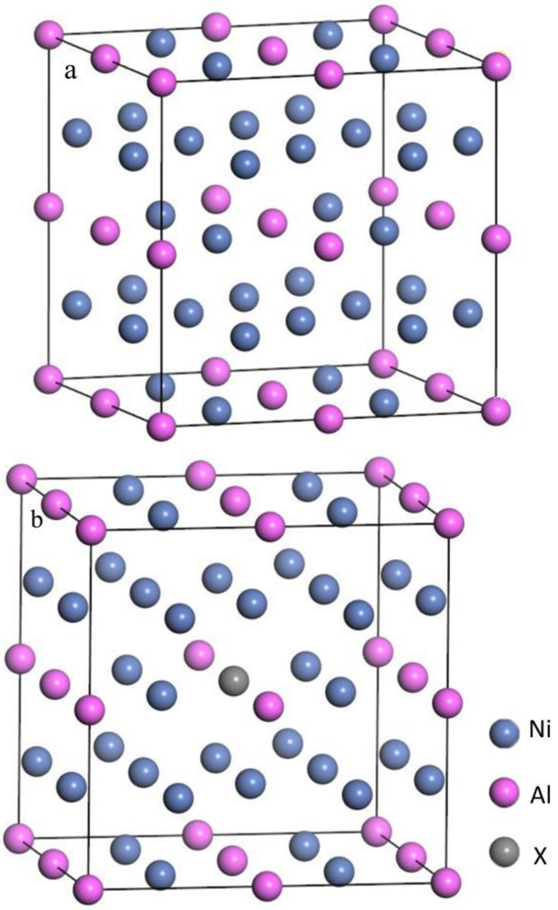

Fig. 2. Super cell model of Ni_3Al alloys used in the calculation: a – original model of Ni_3Al supercell; b – defect model of X (Ni, Ti and Nb) replace Al site

3. RESULTS AND DISCUSSION

3.1. Site preferences of elements in Ni_3Al

Alloying elements M (Ti, Nb) added into the Ni_3Al alloys produce specific defects with the lattice distortion and make the lattice constant larger, and the formation mechanism of which can be described with the substitution formalism and the antisite-based substitution formalism, such as M_{Al}, M_{Ni}, Ni_{Al} and Al_{Ni}. The concentrations of these defects in the Ni_3Al alloy are determined by compositions of alloy and temperature, and formation enthalpies of which can be computed with the Wagner-Schottky model [19] in the dilute limit as follow:

$$\Delta H_f = \Delta H_f(Ni_3Al) + \sum_d H_d x_d, \tag{1}$$

where $\Delta H_f(Ni_3Al)$ is the formation enthalpy per atom for Ni_3Al; x_d is 3.125 at % for anti-site or substitute site in this paper; H_d is the formation enthalpy per defect. In this paper, the ΔH_f of Ni_3Al alloys can be computed according the following reaction equation:

$$\Delta H_f = \frac{E(Ni_xAl_yX_z) - xE(Ni) - yE(Al) - zE(X)}{x + y + z}, \tag{2}$$

where $E(Ni_xAl_yX_z)$ is the total energy of $Ni_xAl_yX_z$, and x, y, z are the number of Ni, Al And X Atom in $Ni_xAl_yX_z$. From the Eq. 1, the formation enthalpy per point defect can be got as follow:

$$H_d = \frac{\Delta H_f - \Delta H_f(Ni_3Al)}{x_d}. \tag{3}$$

The calculation results, including average lattice parameter a(Å), formation enthalpies of alloys ΔH_f (eV/atom) and formation enthalpies per defect H_d (eV/defect), are listed in Table 1, which are in agreement other calculated values [8]. It shows that replace behavior of elements (Al, Ti, Nb) make the lattice constant larger except Ni, and the average lattice parameter of $Ni_{24}Al_7M$ is smaller than $Ni_{23}MAl_8$, which owns to the order of the atomic radius: $r_{Nb}>r_{Ti}>r_{Al}>r_{Ni}$. The formation enthalpies of all alloys are negative, meaning that all of lattice structures are stabilized for Ni_3Al alloys. In binary Ni_3Al alloy, formation enthalpies of vacancy H_d (Va_{Al},Va_{Ni}) [8] are larger than the corresponding formation enthalpies of substitution H_d (Ni_{Al}, Al_{Ni}), signifying that the defects (Ni_{Al}, Al_{Ni}) forming by antisite-based substitution formalism exist in the Ni_3Al alloys. As for the complexity of the point defects forming by the substitution formalism, they can be described by the energy change $E_M^{Ni\to Al}$ (M: Ti, Nb) [20], which is the index to explain the energy required to transfer the alloying atom from a Ni-site to a nearest-neighbor Al site and computed with the following reaction equation:

$$M_{Ni} + Al_{Al} \to M_{Al} + Al_{Ni}. \tag{4}$$

And the energy change $E_M^{Ni\to Al}$ can be calculated in this reaction as follows:

$$E_M^{Ni\to Al} = E(Ni_{24}Al_7M) + E(Ni_{23}AlAl_8) - E(Ni_{23}MAl_8) - E(Ni_{24}Al_8) \tag{5}$$

Table 1. Calculation results of average lattice parameter a (Å), formation enthalpies of alloys ΔHf (eV/atom) and formation enthalpies per defect Hd (eV/defect)

Alloys	Designation	a, Å	a(Å) [8]	ΔHf, eV/atom	ΔHf, eV/atom [8]	Hd	Hd [8]
Ni_3Al	-	3.5772	3.5794	-0.451	-0.4558	-	-
$Ni_{24}Al_7Va$	Va_{Al}	-	-	-	-0.3462	-	3.4
$Ni_{24}Al_7Ni$	Ni_{Al}	3.5746	3.5732	-0.386	-0.3811	2.08	2.39
$Ni_{24}Al_7Ti$	Ti_{Al}	3.5824	3.5838	-0.462	-0.4674	-0.352	-0.37
$Ni_{24}Al_7Nb$	Nb_{Al}	3.5917	3.5903	-0.448	-0.453	0.096	0.09
$Ni_{23}VaAl_8$	Va_{Ni}	-	-	-	-0.4148	-	1.31
$Ni_{23}AlAl_8$	Al_{Ni}	3.6151	3.5881	-0.481	-0.4867	-0.96	-0.99
$Ni_{23}TiAl_8$	Ti_{Ni}	3.6215	3.5947	-0.469	-0.4788	-0.576	-0.74
$Ni_{23}NbAl_8$	Nb_{Ni}	3.6319	3.6043	-0.442	-0.4519	0.288	0.13

The site preferences of elements are predicted in Ni_3Al with the following criterion:

$E_M^{Ni\rightarrow Al} < 0$, M atoms prefer to replace Al site;

$E_M^{Ni\rightarrow Al} > H_{AlNi} + H_{NiAl}$, M atoms prefer to replace Ni sites;

$0 < E_M^{Ni\rightarrow Al} < H_{AlNi} + H_{NiAl}$, M atoms may occupy both sites.

From the Table 1, it can be found that the sum of formation enthalpy of antisite defects in Ni_3Al is 1.12 eV. The calculation results are listed in Table 2, consisting of alloy elements, formation energy factor and corresponding site preferences. Moreover, energy change $E_M^{Ni\rightarrow Al}$ are consistent with the values of other calculation [8] , and all energy change are negative, which means that M (Ti, Nb) replace Al sites in Ni_3Al alloy. The result is also consistent with the other calculation [8, 22].

Table 2. $E_M^{Ni\rightarrow Al}$ value of alloy elements and corresponding site preferences

Alloy elements	$E_M^{Ni\rightarrow Al}$	$E_M^{Ni\rightarrow Al}$ [8]	site preference
Ti	-0.74	-0.62	Al
Nb	-1.13	-1.03	Al

3.2. Elastic properties of polycrystalline alloys

According to the above study, alloying elements M (Ti, Nb) replace Al sites in Ni_3Al alloys, and it is necessary to further study the effect of M on the elastic property of Ni_3Al alloys, which is helpful for alloying design to strengthen Ni_3Al alloy in theory. The elastic deformation of solid is characterized by a reversible strain as a response to the applied stress, and there is a linear relationship satisfied to Hooke's law. For crystal, the force field and the ensuring deformation field have been specified in three dimensions, thus the Hooke's law used for anisotropic crystal can be expressed in tensorial form:

$$\sigma = C\varepsilon \,, \tag{6}$$

where the σ is the stress component applied to the crystal, ε is the corresponding deformation, C is the elastic constant with the dimension of force. Based on the Voigt's theoretical analysis, for the cubic crystal, there is a high degree of symmetry, and the elastic constants matrix of Ni_3Al can be expressed in the 6×6 symmetric matrix:

$$C = \varepsilon^{-1}\sigma = \begin{pmatrix} C_{11} & C_{12} & C_{13} & 0 & 0 & 0 \\ C_{21} & C_{22} & C_{23} & 0 & 0 & 0 \\ C_{31} & C_{32} & C_{33} & 0 & 0 & 0 \\ 0 & 0 & 0 & C_{44} & 0 & 0 \\ 0 & 0 & 0 & 0 & C_{55} & 0 \\ 0 & 0 & 0 & 0 & 0 & C_{66} \end{pmatrix}, \tag{7}$$

where $C_{11} = C_{22} = C_{33}$, $C_{12} = C_{13} = C_{23}$, $C_{44} = C_{55} = C_{66}$.

After doping elements M (Ti, Nb), the symmetry of the cubic system for Ni_3Al is likely broken, thus C_{11}, C_{22} and C_{33} no longer have the same value, as well as C_{12}, C_{13}, C_{23} and C_{44}, C_{55}, C_{66}. Then the average elastic constants are taken into account instead of C_{11}, C_{12} and C_{44}, which have been deemed to be viable to study the elastic properties of alloyed Ni_3Al at present situation [12]:

$$\begin{aligned} \overline{C_{11}} &= (C_{11}+C_{22}+C_{33})/3 \\ \overline{C_{12}} &= (C_{12}+C_{13}+C_{23})/3 \,. \\ \overline{C_{44}} &= (C_{44}+C_{55}+C_{66})/3 \end{aligned} \tag{8}$$

The elastic constants are the basic parameters of solid, after which of Ni_3Al single crystal are calculated by the linear elasticity approximation, some important elastic properties of Ni_3Al polycrystalline alloys can be derived with Voigt-Reuss-Hill approximation [23], such as the bulk (B), shear (G) and young's modulus (E), and which can be computed with the follow standard equations:

$$\begin{aligned} B_V &= B_R = \left(\overline{C_{11}} + 2\overline{C_{12}}\right)/3 \\ B_H &= (B_V + B_R)/2 \end{aligned} \tag{9}$$

$$G_V = \left(\overline{C_{11}} - \overline{C_{12}} + 3\overline{C_{44}}\right)/5 \qquad G_R = \left[\frac{4}{5}\left(\overline{C_{11}} - \overline{C_{12}}\right)^{-1} + \frac{3}{5}\overline{C_{44}}^{\,-1}\right]^{-1}$$

$$G_H = (G_V + G_R)/2 \,; \tag{10}$$

$$E_H = \frac{9B_H G_H}{3B_H + G_H} \,. \tag{11}$$

The calculated elastic properties of pure Ni_3Al and $Ni_{24}Al_7M$ are shown in the Table 3, including average elastic constants of Ni_3Al single crystal, bulk modulus B, shear modulus G, Young's modulus E and the bulk/shear modulus ratio (B/G) of Ni_3Al polycrystalline alloys. All average elastic constants are in agreement with other calculation values [8, 9] and experimental values [10, 24], meaning that the given computing models and parameters are reasonable. In fact, the elastic constants are applied to stability judgment for crystals sometimes, combining with the born stability criteria [25], Ni_3Al, $Ni_{24}Al_7Ti$ and $Ni_{24}Al_7Nb$ are considered to be mechanically stable phases. From the Table 3, it is found that the bulk modulus B of Ni_3Al alloy increases with the M (Ti, Nb) doping, and the B values of Ni_3Al, $Ni_{24}Al_7Ti$ and $Ni_{24}Al_7Nb$ respectively are 181.5 GPa, 184.4 GPa, 187.1 GPa. While $Ni_{24}Al_7Nb$ has the largest bulk modulus B, suggesting that the average bond strength of atoms for $Ni_{24}Al_7Nb$ is the strongest in all alloys. The shear modulus G is more meaningful to resistance of dislocation motion than the bulk modulus B, and the shear modulus G of Ni_3Al is 81.13 GPa, with the M doping, the G of corresponding alloy $Ni_{24}Al_7M$ is larger than Ni_3Al, and the shear modulus G of $Ni_{24}Al_7Nb$ is largest, meaning that the ability to resist plastic deformation of $Ni_{24}Al_7Nb$ is better than others. Young's modulus E can be used as the evaluation of the stiffness of solid. On the basis of fact that elements M (Ti, Nb) increases Young's modulus of Ni_3Al alloy, thus stiffness of Ni_3Al alloy with M doping can be improved as well.

Pugh [26] pointed out that the bulk/shear modulus ratio (B/G) could evaluate the brittleness/ ductility of alloy, while the ductility of alloy increased with the increase of ratios. The alloy possesses ductility when B/G value is larger than 1.75, otherwise, which possesses brittleness. As showed in Table 3, the ratio values of Ni_3Al, $Ni_{24}Al_7Ti$ and $Ni_{24}Al_7Nb$ respectively are 2.24, 2.16 and 2.16, all of which are larger than 1.75, signifying that the Ni_3Al, $Ni_{24}Al_7Ti$ and $Ni_{24}Al_7Nb$ polycrystalline alloys possess ductility. Moreover, the B/G values of $Ni_{24}Al_7Ti$ is similar to $Ni_{24}Al_7Nb$, and all of which are smaller than Ni_3Al, indicating that $Ni_{24}Al_7Ti$ and $Ni_{24}Al_7Nb$ polycrystalline alloys are more brittle than Ni_3Al polycrystalline alloy.

3.3. Electronic structure

To understand the electronic structure of Ni_3Al and $Ni_{24}Al_7M$, and elastic properties change of Ni_3Al with M (Ti, Nb) doping, the supercell and the valence electrons (Al 3s2 3p1, Ni 3d8 4s2, Ti 3s2 3p6 3d2 4s2 and Nb 4s2 4p6 4d4 5s1) are used to compute the total density of states (TDOS), partial density of states (PDOS), electron density difference and Mulliken population in Ni_3Al alloys.

Fig. 3 shows the density of states DOS (TDOS, PDOS) of $Ni_{24}Al_8$ (Ni_3Al) and $Ni_{24}Al_7M$. The dotted line lied in zero-point energy represents the Fermi level (E_F). Fig. 3 a shows that the valence band of the $Ni_{24}Al_8$ is distributed in the -10-0 eV region. The lower valence band between -10 to -5 eV is mainly contributed by the Al-3s and Al-3p orbital, and the upper valence band between -5 to 0 eV is mainly contributed by the Al-3s orbital and Ni-3d orbital. The valence bands of the Ni_3Al doped with the M (Ti, Nb) are showed in Fig. 3 b and c, which are divided into three regions, the lower valence band (from-53.5 to -57.5 eV), the middle valence band (from -30 to -35 eV), the upper valence band (from -10 to 0 eV).

The lower valence band is contributed by the weakly interaction between M-s orbital and Ni-4s orbital, the middle valence band is contributed by the M-p (Ti-3p, Nb-4p) orbital, and the upper valence band is contributed by the orbital hybridization between Al-3p orbital, Ni-3d orbital and M-d (Ti-3d, Nb-4d) orbital. As shown in Fig. 3, TDOS at Fermi level are not zero, meaning metallic-like behavior for Ni_3Al, $Ni_{24}Al_7Ti$ and $Ni_{24}Al_7Nb$. Moreover, the position of Fermi level in TDOS curve can be used to judge the structural stability of the compounds. Ni_3Al, $Ni_{24}Al_7Nb$ and $Ni_{24}Al_7Ti$ are stable phases due to the Fermi level lies around the valley of TDOS. Fig. 4 shows electron density difference of $Ni_{24}Al_8$ and $Ni_{24}Al_7M$ along $(1\bar{1}0)$ plane. Electron density difference describes the direction and extent of electron transfer of atoms in $Ni_{24}Al_8$ and $Ni_{24}Al_7M$. The high electron density region (the deep color region) is correspond to core of the Ni, Al, Ti and Nb atoms, and the range of charge density values is $-5\times10^{-2}\sim5\times10^{-2}$ e/Å^3 for $Ni_{24}Al_8$ and $Ni_{24}Al_7M$. The area of red stands for losing electrons and the area of blue stands for getting the electrons. The charges have transferred between the adjacent atoms of Ni-(Al, Nb and Ti), it means that the Ni-Al is covalent bond, as well as Ni-Nb and Ni-Ti. Even though there are no obvious charge transfers between adjacent atoms Al-Al and Ni-Ni, a large number of charges exist in the region between Al atoms and Ni atoms, meaning that covalent character exists in Al–Al and Ni-Ni bonds. Furthermore, after the Ni_3Al doped with the transition elements M (Ti, Nb), as the Fig. 4 b and c showed, the charges transfer between adjacent atoms Ni-M are more than Ni-Al, indicating that the covalence of Ni-M is stronger than Ni-Al, and the covalence of Ni-Nb is most obvious in all adjacent atoms, so M (Ti, Nb) doping in Ni_3Al alloy can increase their elasticity modulus and the $Ni_{24}Al_7Nb$ has the biggest elasticity modulus.

Table 3. The calculated elastic properties (GPa) of pure Ni_3Al and $Ni_{24}Al_7M$

Designation	$\overline{C_{11}}$	$\overline{C_{12}}$	$\overline{C_{44}}$	B	G	E	B/G	Ref
Ni_3Al	236.07	154.24	127.94	181.5	81.1	211.8	2.24	Cal
	243.8	148.7	123.4	180.4	84.2	218.5	2.14	[8]
	242.0	152.0	125.0	182.0	83.0	217.0	2.18	[9]
	230±5	151±5	126±5	178±5	92	-	-	[10]
	233.0	152.0	107.0	179.0	73.0	-	-	[24]
$Ni_{24}Al_7Ti$	250.9	151.1	122.2	184.4	85.3	221.7	2.16	Cal
	246.8	148.8	128	181.5	87.1	225.3	2.08	[8]
$Ni_{24}Al_7Nb$	255.2	153	123.3	187.1	86.6	225.1	2.16	Cal
	249.8	152.4	125.5	184.9	86	223.3	2.15	[8]

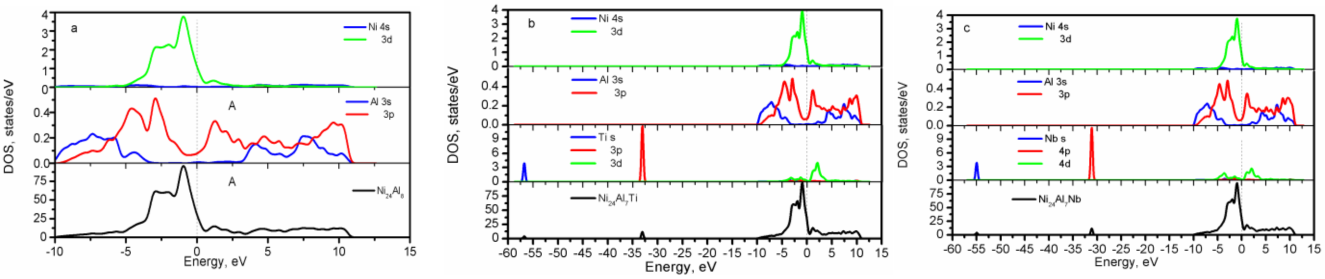

Fig. 3. The the density of states DOS (TDOS, PDOS) of $Ni_{24}Al_8$ and $Ni_{24}Al_7M$: a – DOS of $Ni_{24}Al_8$; b– DOS of $Ni_{24}Al_7Ti$; c– DOS of $Ni_{24}Al_7Nb$

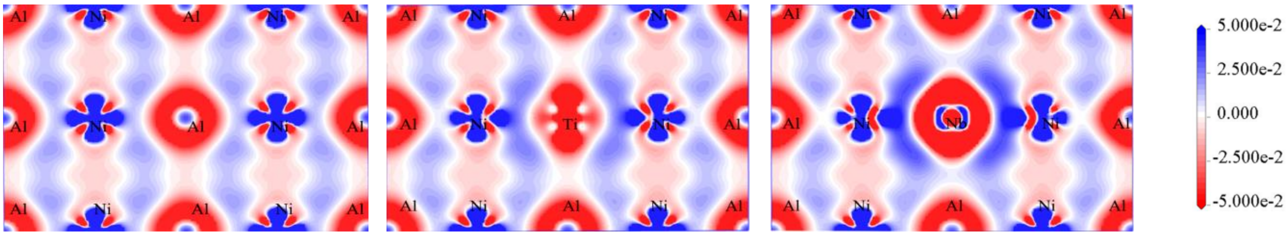

a b c

Fig. 4. Electron density difference of $Ni_{24}Al_8$ and $Ni_{24}Al_7M$ along$(1\ \bar{1}\ 0)$ plane: a– $Ni_{24}Al_8$; b– $Ni_{24}Al_7Ti$; c– $Ni_{24}Al_7Nb$

Table 4. Mulliken population of $Ni_{24}Al_8$ and $Ni_{24}Al_7M$ (using the arithmetic average values)

phase	Ions	s	p	d	Total	Charge (e)
$Ni_{24}Al_8$	Al	3s-0.88	3p-1.87	0	2.75	+0.25
	Ni	4s-0.49	4p-0.83	3d-8.76	10.08	-0.08
$Ni_{24}Al_7Ti$	Al	3s-0.881	3p-1.88	0	2.76	+0.24
	Ti	3s,4s-2.37	3p-6.41	3d-2.6	11.39	+0.61
	Ni	4s-0.5	4p-0.835	3d-8.76	10.095	-0.095
$Ni_{24}Al_7Nb$	Al	3s-0.886	3p-1.884	0	2.77	+0.23
	Nb	4s,5s-2.47	4p-5.53	4d-3.91	11.91	+1.09
	Ni	4s-0.51	4p-0.835	3d-8.765	10.11	-0.11

In addition, the shape of the electron density is petal around the Ni atom and the Ti atom, indicating that the shape electron density of Ti and Ni are more anisotropy than Nb and Al.

In order to furtherly obtain distribution and transfer of the electrons among atoms, the average electron Mulliken population of $Ni_{24}Al_8$, $Ni_{24}Al_7Ti$ and $Ni_{24}Al_7Nb$ are calculated, as showed in the Table 4. The symbol (+) stands for losing charges and (-) stands for getting the charges, showing that the direction of charge transfer in adjacent atoms and different orbitals of the same atom. The bonds of adjacent atoms in the $Ni_{24}Al_7Nb$ and $Ni_{24}Al_7Ti$ are mainly contributed by the reaction of the Al-3s, 3p electrons, Ni-3d electrons and M-d (Ti-3d, Nb-4d) electrons, which also is consistent with the results of the analysis of the electronic density states. Moreover, the electrons transfer is 0.25 e from the Al to Ni in $Ni_{24}Al_8$, after doping the M (Ti, Nb) in $Ni_{24}Al_8$, the charge of Al has few changed and the charges can transfer to Ni from M (Ti, Nb), which is 0.61e from the Ti to Ni in $Ni_{24}Al_7Ti$ and 1.09e from the Nb to Ni in $Ni_{24}Al_7Nb$. Obviously, the Nb and Ti transfer more charges than Al and which of Nb transfer is the most, indicating that the covalence of Ni-Nb and Ni-Ti are stronger than Ni-Al and the covalence of Ni-Nb is strongest, which is consistent with the analysis of electron density difference for Ni_3Al and $Ni_{24}Al_7M$.

4. CONCLUSIONS

The site preferences and elastic properties of M (Ti, Nb) doping in Ni_3Al are predicted and electronic structure are analyzed with CASTEP based on the first principles. It is found that lattice constants of Ni_3Al get larger with doping M (Ti, Nb) due to which replaces Al sites. The bulk modulus B, shear modulus G and Young's modulus E of Ni_3Al polycrystalline alloy increase with M (Ti, Nb) doping and $Ni_{24}Al_7Nb$ has the largest B (187.1 GPa), G (86.6 GPa) and E (225.1 GPa). The bulk/shear modulus ratios (B/G) of Ni_3Al alloy decrease with M (Ti, Nb) doping, while B/G are larger than 1.75, it means that Ni_3Al, $Ni_{24}Al_7Nb$ and $Ni_{24}Al_7Ti$ polycrystalline alloys possess ductility. Analysis of results of electronic structure shows that the main interaction between the Ni atoms and the Al atoms is covalence in the Ni_3Al, after doping elements M (Ti, Nb) in Ni_3Al, there is strong orbital hybridization between the Al-3p orbital, Ni-3d orbital and M-d (Ti-3d, Nb-4d) orbital. The Nb and Ti provide more charges to share with Ni than Al provides and which of Nb provides is the most, indicating that there is a stronger covalent bond between Ni atom and M (Ti, Nb) atom than which between Al and Ni adjacent atoms, and covalent bond between Nb atom and Ni atom is the strongest.

Acknowledgment

The project was supported by Chongqing common key technological innovation of key industries project (cstc2015zdcy-ztzx50002), The National Key Research and Development Program of China (Grant No.2016YFB0402602), National Natural Science Foundation of China (No.51401039) and Chongqing Research Program of Basic Research and Frontier Technology (CSTC2013jcyjA50016).

REFERENCES

1. **Reed, R.C.** The Superalloys: Fundamentals and Applications Cambridge University Press, London, 2006. https://doi.org/10.1017/CBO9780511541285
2. **Warnken, N., Larsson, H., Reed, R.C.** Coupled Modelling of Solidification and Solution Heat Treatment of Advanced Single Crystal Nickel Base Superalloy *Materials Science & Technology* 25 (2) 2009: pp. 179 – 185.
3. **Sikka, V.K., Deevi, S.C., Viswanathan, S.** Advances in Processing of Ni3Al-Based Intermetallics and Applications *Intermetallics* 8 (9 – 11) 2000: pp. 1329 – 1337.
4. **Sikka, V.K., Mavity, J.T., Anderson, K.** Processing of Nickel Aluminides and Their Industrial Applications *Materials Science and Engineering: A* 153(1 – 2) 1992: pp. 712 – 721.
5. **Aoki, K., Ishikawa, K., Masumoto, T.** Ductilization of Ni3Al by Alloying with Boron and Substitutional Elements *Materials Science and Engineering: A* 192–193(1) 1995: pp. 316 – 323.
6. **Soga, W., Kaneno, Y., Takasugi, T.** Phase Relation and Microstructure in Multi-Phase Intermetallic Alloys Based on Ni_3Al–Ni_3Nb–Ni_3V Pseudo-Ternary Alloy System *Intermetallics* 14 (2) 2006: pp. 170 – 179.
7. **Tomihisa, K., Kaneno, Y., Takasugi, T.** Phase Relation and Microstructure in Multi-Phase Intermetallic Alloys Based On Ni_3Si–Ni_3Ti–Ni_3Nb Pseudo-Ternary Alloy System *Intermetallics* 12 (3) 2004: pp. 317 – 325.
8. **Wu, Q., Li, S.** Alloying Element Additions to Ni_3Al: Site Preferences and Effects on Elastic Properties from First-Principles Calculations *Computational Materials Science* 53 (1) 2012: pp. 436 – 443. https://doi.org/10.1016/j.commatsci.2011.09.016
9. **Kim, D.E., Shang, S.L., Liu, Z.K.** Effects of Alloying Elements on Elastic Properties of Ni_3Al by First-Principles Calculations *Intermetallics* 18 (6) 2010: pp. 1163 – 1171.
10. **Kumar, A., Chernatynskiy, A., Hong, M., Phillpot, S.R., Sinnott, S.B.** An ab Initio Investigation of the Effect of Alloying Elements on the Elastic Properties and Magnetic Behavior of Ni_3Al *Computational Materials Science* 101 2015: pp. 39–46. https://doi.org/10.1016/j.commatsci.2015.01.007
11. **Mrunalkumar, C., Jaimie, T., Rajarshi, B., Du, J.C.** Site Preference and Interaction Energies of Co and Cr in Gamma Prime Ni_3Al: A First-Principles Study *Modelling and Simulation in Materials Science and Engineering* 21 (5) 2013: pp. 55 – 66.
12. **Zhao, W.Y, Sun, Z.M., Gong, S.K.** Synergistic Effect of Co-Alloying Elements on Site Preferences and Elastic Properties of Ni_3Al: A First-Principles Study *Intermetallics* 65 2015: pp. 75 – 80.
13. **Cermak, J., Rothova, V.** Concentration dependence of Ternary Interdiffusion Coefficients in Ni_3Al/Ni_3Al–X Couples with X=Cr, Fe, Nb and Ti *Acta Materialia* 51 2003: pp. 4411 – 4421. https://doi.org/10.1016/S1359-6454(03)00276-3
14. **Ohira, K., Kaneno, Y., Takasugi, T.** Microstructure, Mechanical Property and Chemical Property in Ni3Al-Ni3Ti-Ni3Nb-Based Multi-Intermetallic Alloys *Journal of Materials Science* 39 2004: pp. 2295 – 2301. https://doi.org/10.1023/B:JMSC.0000019990.75927.aa
15. **Mohan Rao, P.V., Murthy, K.S., Suryanarayana, S.V., Naidu, S.V.N.** Effect of Ternary Additions on the Room Temperature Lattice Parameter of Ni_3Al *Physica Status Solidi* 133 (133) 1992: pp. 231 – 235. https://doi.org/10.1002/pssa.2211330203
16. **Clark, S.J., Segall, M.D., Pickard, C.J. Hasnip, P.J., Probert, M.I.J., Refson, K., Payne, M.C.** First Principles Methods using CASTEP *Zeitschrift Für Kristallographie* 220 (5 – 6) 2005: pp. 567 – 570.
17. **Perdew, J.P., Burke, K., Ernzerhof, M.** Errata: Generalized Gradient Approximation Made Simple *Physical Review Letters* 77 (18) 1996: pp. 3865 – 3868. https://doi.org/10.1103/PhysRevLett.77.3865
18. **Fischer, T.H., Almlof, J.** General Methods for Geometry and Wave Function Optimization *Journal of Physical Chemistry* 96 (24) 1992: pp. 9768 – 9774.
19. **Korzhavyi, P.A., Ruban, A.V., Lozovoi, A.Y., Vekilov, Y.K., Abrikosov, I.A., Johansson, B.** Constitutional and Thermal Point Defects in B2 NiAl *Physical Review B* 61 (9) 2000: pp. 6003 – 6018. https://doi.org/10.1103/PhysRevB.61.6003
20. **Ruban, A.V., Skriver, H.L.** Calculated Site Substitution in γ'-Ni_3Al *Solid State Communications* 99 (11) 1996: pp. 813 – 817. https://doi.org/10.1016/0038-1098(96)00279-7
21. **Chaudhari, M., Singh, A., Gopal, P., Nag, S., Viswanathan, G.B., Tiley, J.** Site Occupancy of Chromium in the γ'-Ni_3Al Phase of Nickel-based Superalloys: a Combined 3d Atom Probe and First-principles Study *Philosophical Magazine Letters* 92 (9) 2012: pp. 495 – 506.
22. **Jiang, C., Gleeson, B.** Site Preference of Transition Metal Elements in Ni_3Al *Scripta Materialia* 55 (5) 2006: pp. 433 – 436. https://doi.org/10.1016/j.scriptamat.2006.05.016
23. **Hill, R.** The Elastic Behaviour of a Crystalline Aggregate *Proceedings of the Physical Society* 65 (5) 1952: pp. 349 – 354.
24. **Rinkevich, A.B., Stepanova, N.N.** Acoustical Properties of Ni_3Al Single Crystals Alloyed with Cobalt and Niobium *The Physics of Metals and Metallography* 102 (6) 2006: pp. 632 – 636.
25. **Born, M.** Thermodynamics of Crystals and Melting *Journal of Chemical Physics* 7(8) 1939: pp. 591 – 603.
26. **Pugh, S.F.** Relations Between the Elastic Moduli and the Plastic Properties of Polycrystalline Pure Metals *Philosophical Magazine* 45 (367) 1954: pp. 823 – 843.